Asymmetry Dependence of Proton Correlations

R. J. Charity,[1] L. G. Sobotka,[1,2] and W. H. Dickhoff[2]
[1]Department of Chemistry, Washington University, St. Louis, Missouri 63130, USA
[2]Department of Physics, Washington University, St. Louis, Missouri 63130, USA
(Received 19 May 2006; published 17 October 2006)

A dispersive-optical-model analysis of $p + {}^{40}$Ca and $p + {}^{48}$Ca interactions has been carried out. The real and imaginary potentials have been constrained from fits to elastic-scattering data, reaction cross sections, and level properties of valence hole states deduced from $(e, e'p)$ data. The surface imaginary potential was found to be larger overall and the gap in this potential on either side of the Fermi energy was found to be smaller for the neutron-rich $p + {}^{48}$Ca system. These results imply that protons with energies near the Fermi surface experience larger correlations with increasing asymmetry.

DOI: 10.1103/PhysRevLett.97.162503 PACS numbers: 21.10.Pc, 24.10.Ht, 25.30.Dh, 25.40.Cm

In the independent-particle model, nucleons in the nucleus move in a mean-field potential generated by the other nucleons. All nucleon levels with energies up until the Fermi energy (E_F) are fully occupied, while those above are empty. Although this model enables an understanding of various aspects of nuclear structure, a full description of nuclei and nuclear matter requires consideration of the correlations between the nucleons. These include short-range, central and tensor interactions, and longer range correlations associated with low-lying collective excitations [1,2]. As a result, for closed-shell nuclei, single-particle (SP) levels below E_F have an occupancy of only 70%–80% and the levels at higher energy have a nonzero occupancy [3]. The strength of the SP levels is spread over energy, with narrow peaks or broad distributions (depending on their separation from E_F). In addition, there is strength at very high momentum [4].

Although there are numerous studies of the effect of correlations on the properties of SP levels for nuclei near stability, there are only a few studies for very neutron or proton-rich nuclei. From neutron knockout reactions, Gade *et al.* [5] infer the occupancy of the $0d_{5/2}$ neutron hole state in the proton-rich ^{32}Ar nucleus is considerably reduced relative to those for stable nuclei.

An alternate method to study SP strength is through the use of the dispersive-optical model (DOM) developed by Mahaux and Sartor [6]. This description employs the Kramers-Kronig dispersion relation that links the imaginary and real parts of the nucleon self-energy [7]. This procedure links optical-model (OM) analyses of reaction data at positive energies to structural information at negative energies. In the present work, the properties of proton levels in Ca nuclei as a function of asymmetry $\delta = \frac{N-Z}{A}$ are investigated with the DOM. Previously measured elastic-scattering and reaction-cross-section data for protons on ^{40}Ca and ^{48}Ca, as well as level properties of hole states in these nuclei, inferred from $(e, e'p)$ reactions, were simultaneously fit. The dependence on δ is extracted and used to predict level properties of ^{60}Ca.

In the DOM, the complex energy-dependent potential felt by the protons is comprised of a real $\mathcal{V}$, volume W_v, and surface W_s imaginary components, plus spin-orbit V_{SO} and Coulomb V_c potentials,

$$\mathcal{U}(r, E) = -\mathcal{V}(r, E) + V_{so}(r) + V_c(r) - iW_v(E) f(r, r_v, a_v) + 4ia_s W_s(E) \times \frac{d}{dr} f(r, r_s, a_s). \quad (1)$$

Wood-Saxon form factors $f(r, r_i, a_i) = [1 + e^{(r - r_i A^{1/3}/a_i)}]^{-1}$ are used. The real part of the nuclear potential is assumed to be given by two terms

$$\mathcal{V}(r, E) = V_{\rm HF}(E) f(r, r_{\rm HF}, a_{\rm HF}) + \Delta\mathcal{V}(r, E), \quad (2)$$

where $V_{\rm HF}$ has a smooth energy dependence arising from the nonlocality or momentum-dependence of the microscopic self-energy. The dispersive correction $\Delta\mathcal{V}$ has volume and surface parts,

$$\Delta\mathcal{V}(r, E) = \Delta V_v(E) f(r, r_v, a_v) - 4a_s \Delta V_s(E) \times \frac{d}{dr} f(r, r_s, a_s), \quad (3)$$

and is related to the imaginary potential through the dispersion relationship, i.e.,

$$\Delta V_i(E) = \frac{P}{\pi} \int_{-\infty}^{\infty} W_i(E') \left(\frac{1}{E' - E} - \frac{1}{E' - E_F} \right) dE', \quad (4)$$

where $i = v$, s, and P stands for the principal value. The dispersive corrections are a result of coupling to nonelastic channels. The surface term accounts for the influence of low-lying collective states and giant resonances.

The form for the imaginary potential must take into account the dominance of surface and volume absorption at low and high positive energies, respectively. In addition, around E_F the imaginary potentials must be zero. The potential should be approximately symmetric around E_F, but further away it must become asymmetric as there are a

finite number of hole states. In this Letter we assume

$$W_v(E) = A_v \frac{(E - E_F)^4}{(E - E_F)^4 + B_v^4} + \Delta W_{\rm NM}(E), \qquad (5)$$

where the energy-asymmetric correction $\Delta W_{\rm NM}(E)$ is derived from nuclear-matter considerations [6]. The surface potential was taken as the difference of two functions that cancel at large energies, i.e.,

$$W_s(E) = \omega_4(E, A_s^1, B_s^1, c, 0) - \omega_2(E, A_s^2, B_s^2, c, Q), \qquad (6)$$

$$\omega_n(E, A_s, B_s, c, Q) = A_s \Theta(X) \frac{X^n}{X^n + B_s^n} e^{-cX}, \qquad (7)$$

where $\Theta(X)$ is Heavyside's step function, $X = |E - E_F| - Q$, $A_s^2 = A_s^1 e^{-cQ}$, and $Q = B_s^1 + \Delta B$.

The Hartree-Fock potential is often assumed to decrease linearly or exponentially with energy. We took the form

$$V_{\rm HF}(E) = \frac{2A_{\rm HF}}{1 + \exp[B_{\rm HF}(E - E_F)/A_{\rm HF}]}, \qquad (8)$$

which is approximately linear around E_F and becomes more exponential at larger energies. This form provided a reasonable location for the $0s_{1/2}$ level in ^{40}Ca.

The parameters of the DOM were fit for both ^{40}Ca and ^{48}Ca from a large set of data covering both positive and negative proton energies. For ^{40}Ca, 14 experimental elastic-scattering angular distributions for energies from 18 to 135 MeV [8–13] and seven data sets for the analyzing power measured at energies from 21 to 80 MeV [12,14–18] were included. For ^{48}Ca the fitted data included 14 angular distributions and seven sets of analyzing power at energies from 8 to 65 MeV [12,13,19,20]. Reaction cross sections for both targets were taken from the tabulations of Bauhoff [21]. For the $0d_{5/2}$, $1s_{1/2}$, and $0d_{3/2}$ proton holes states, the mean level energies, rms radii, spectroscopic factors, and widths inferred from measured $(e, e'p)$ cross sections [22,23] were also included. Lastly, the fits considered the mean energies of the $0f_{7/2}$ and $0f_{5/2}$ (for ^{48}Ca only) particle levels [24].

The seven geometric parameters ($r_{\rm HF}$, $a_{\rm HF} = a_v$, r_v, r_s, a_s, $r_{\rm so}$, $a_{\rm so}$) defining the form factors were varied, but kept identical for both targets. Similarly, the fit parameters B_s^2, ΔB, and c, defining the decay of the $W_s(E)$ at large energies, as well the magnitude of the spin-orbit term, were also set identical for both targets. Only $A_{\rm HF}$, $B_{\rm HF}$, A_s^1, B_s^1, A_v, and B_v were allowed to differ for each isotope.

The final fit to the experimental data is shown in Figs. 1–3, the parameters are listed in Table I, and the potentials are displayed in Fig. 4(a). It was found possible to obtain similar quality fits with different potentials, however, a robust feature *of all good fits* was that the magnitude of the surface imaginary potential (A_s^1) was larger and the width B_s^1 (of the minimum around E_F) was narrower for the neutron-rich ^{48}Ca nucleus. There was, however, an ambiguity in determining the rate at which this potential diminished at large energies. This ambiguity is coupled with an ambiguity in determining the magnitude and the rate of increase of $W_v(E)$.

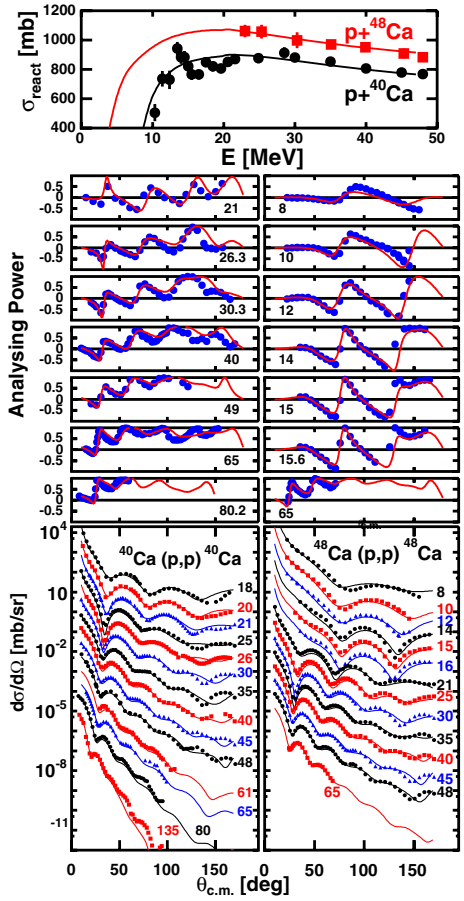

FIG. 1 (color online). Calculated and experimental reaction cross sections $\sigma_{\rm react}$ and elastic-scattering angular distributions of the differential cross section $d\sigma/d\Omega$ and analyzing power. Left panels shows results for $p + {}^{40}$Ca, right for $p + {}^{48}$Ca. Each curve is labeled by the proton energy in MeV. For display purposes, successively higher-energy curves and data for $d\sigma/d\Omega$ are scaled down by an additional factor of 4.5. For the lowest energies, compound-elastic contributions were also included in the fits.

Tornow *et al.* [25] fitted similar data for ^{40}Ca with the DOM using a $W_s(E)$, which decreased slowly and was still substantial at the highest energy considered in the work. With such a slow diminishing of $W_s(E)$, one can also obtain good fits to the ^{48}Ca data, however the fitted $W_v(E)$ potentials are substantially different for ^{40}Ca and ^{48}Ca. On the other hand, if $W_s(E)$ is made to diminish faster, these differences can be reduced to zero.

Ambiguities in determining potentials in standard OM fits are well known, however volume integrals of the potentials have been shown to be better defined [6]. Comparisons of the imaginary volume integral, $J_W(E) = \int W(r, E) d\mathbf{r}$, obtained from the OM fits in the referenced experimental studies, indicate that J_W is larger below

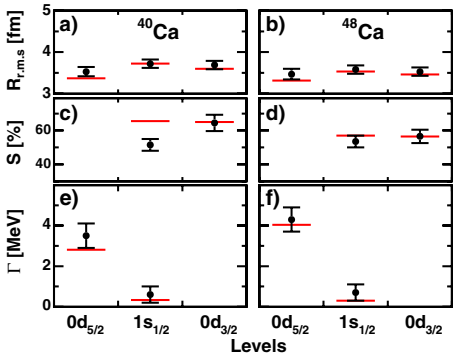

FIG. 2 (color online). Fitted level properties for the $0d_{5/2}$, $1s_{1/2}$, and $0d_{3/2}$ proton hole states. The left (a),(c),(e) and right (b),(d),(f) panels display the fits for ^{40}Ca and ^{48}Ca, respectively. The fitted quantities include (a),(b) the root-mean-squared radius $R_{\rm rms}$, (c),(d) the spectroscopic factor S expressed as a percent of the independent-particle-model value, and (e),(f) the widths Γ of these levels.

$E \sim 50$ MeV in ^{48}Ca. However for higher energies, there is no discernible difference for the two isotopes. Thus for ^{48}Ca, if its larger surface potential is still significant in this higher-energy region, $W_v(E)$ must be smaller to produce similar values of J_W. We believe this result is artificial, and therefore a solution where $W_s(E)$ diminishes faster is preferable. In any case, the present analysis cannot constrain any difference in $W_v(E)$ for the two nuclei. Thus, for the final fit we have taken $W_v(E)$ to be independent of asymmetry. This is consistent with global OM fits [26] which have a significant asymmetry dependence for $W_s(E)$, but none for $W_v(E)$. Theoretically some asymmetry dependence of $W_v(E)$ would be expected and higher-energy ^{48}Ca data may provide sensitivity to this.

Calculated and experimental SP level schemes for ^{40}Ca and ^{48}Ca are displayed in Fig. 3. Apart from the levels included in the fit (indicated with the solid dots), the other known levels are well reproduced. The $0s_{1/2}$ level of ^{40}Ca

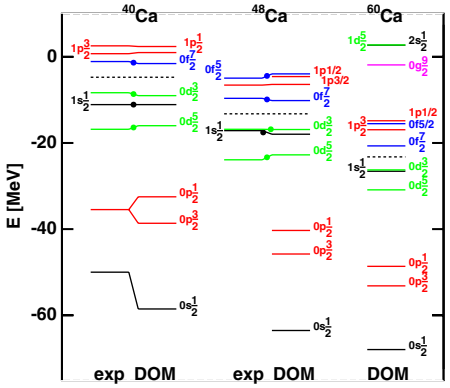

FIG. 3 (color online). Comparison of experimental proton single-particle levels [22–24,27,30–32] to DOM calculations. For the levels indicated with the solid dots, their energies were included in the fits. The dashed lines indicate the Fermi energy.

TABLE I. Values of the fitted geometric parameters in fm and the fitted potential parameters in MeV.

$r_{\rm HF} = 1.16$, $a_{\rm HF} = a_v = 0.67$, $r_s = 1.19$, $a_s = 0.61$
$r_v = 1.36$, $r_{\rm so} = 0.97$, $a_{\rm so} = 0.67$, r_C(fixed) $= 1.31$
$V_{SO} = 6.57$, $1/c = 67.1$, $B_s^2 = 35.03$, $\Delta B = 14.84$
$A_{\rm HF} = 61.55_{40}, 67.41_{48}$, $B_{\rm HF} = 0.624_{40}, 0.574_{48}$, $A_v = 9.95$
$A_s^1 = 10.83_{40}, 14.94_{48}$, $B_s^1 = 15.57_{40}, 12.25_{48}$, $B_v = 57.84$

is very wide and even though the DOM prediction for its energy is low, it lies within the experimentally determined width [27].

Present DOM calculations have been extrapolated to ^{60}Ca assuming the parameters $A_{\rm HF}$, $B_{\rm HF}$, A_s^1, and B_s^1 vary linearly with δ. The extrapolated energy-dependence of $W_s(E)$ is shown in Fig. 4(a) and the predicted SP level scheme is displayed in Fig. 3. The surface dispersive correction is now large and produces the following effects. The levels in the immediate vicinity of E_F are focused closer to E_F, increasing the density of SP levels. A reduced gap between the particle and hole valence levels implies that the closed-shell nature of this nucleus has diminished and proton pairing may be important. The levels further from E_F have been pushed away and as a result there are big gaps between the $0p_{1/2}$ and the $0d_{5/2}$ and also the $1p_{1/2}$ and $0g_{9/2}$ levels.

The occupation probabilities as defined in Ref. [6] are plotted in Fig. 4(c). These results are sensitive to the assumed form of $\Delta W_{\rm NM}$ in Eq. (5). Refitting the data with this term set to zero, increases the extracted occupations by 7% for hole states and by a smaller amount for

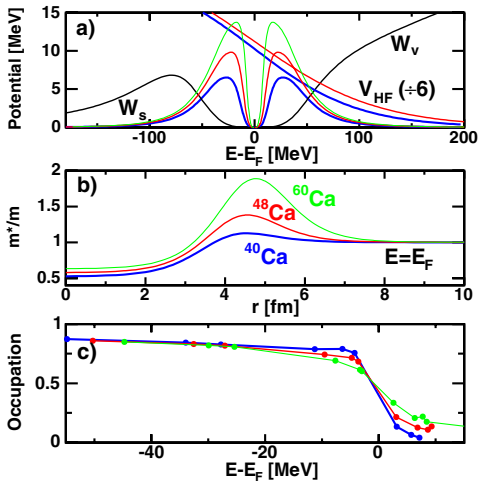

FIG. 4 (color online). Quantities derived from DOM fits. (a) The energy dependence of the Hartree-Fock potential $V_{\rm HF}$, and the surface W_s and volume W_v imaginary potentials. (b) The radial dependence of the effective mass at E_F. (c) The occupation probabilities (points indicate SP levels). For all plots, the thick (back), medium (red), and thin (green) curves give the results for ^{40}Ca, ^{48}Ca, and ^{60}Ca, respectively.

particle states. However, the relative change in occupations between the two targets show much less sensitivity to ΔW_{NM}. The results for ^{48}Ca agree with the theoretical work of Ref. [28]. For proton hole states just below E_F, the occupation probabilities have decreased for the more neutron-rich ^{48}Ca while the opposite is true for the particle states. This trend is further accentuated in our extrapolation to ^{60}Ca. On the other hand, the more deeply-bound $0s_{1/2}$, $0p_{3/2}$, and $0p_{1/2}$ levels show very little sensitivity. Their occupancies are more sensitive to the volume imaginary component whose asymmetry dependence was not constrained.

Our observation that the occupancies of valence proton hole states are reduced in neutron-rich ^{48}Ca can be compared to the reduced occupancy of the valence neutron hole state in the proton-rich ^{32}Ar inferred by Gade *et al.* [5]. Thus a preponderance of one type of particle reduces the occupancies of valence hole states for the other type. This indicates that correlations are stronger for these valence nucleons. Recent calculations of asymmetric nuclear matter by Frick *et al.* [29] also predict such a result as a purely volume effect. Its origin is probably similar in both cases reflecting that p-n interactions are stronger than n-n or p-p, partly because of the tensor force. Thus, protons in neutron-rich systems are more strongly correlated as illustrated from the inferred spectroscopic factors of 65%, 56%, and 50% for the $0d_{3/2}$ proton level in ^{40}Ca, ^{48}Ca, and ^{60}Ca, respectively. Conversely for neutrons, the opposite is expected.

The nucleon effective mass $m^*(r, E)/m = 1 - dV(r, E)/dE$ (m is the nucleon mass) at $E = E_F$ inferred from this work is displayed in Fig. 4(b). Only the surface contribution around $r = 4$–5 fm has been constrained and it increases significantly with asymmetry. This suggests an asymmetry dependence of the surface component of the level-density parameter.

In conclusion, the properties of proton single-particle states in the vicinity of E_F for ^{40}Ca and ^{48}Ca have been studied with a comprehensive dispersive-optical-model analysis of elastic-scattering and bound-level data. The analysis indicates that the imaginary surface potential is $\sim$50% larger and the minimum around the Fermi energy is narrower for the neutron-rich ^{48}Ca nucleus. This implies that, with increasing asymmetry, the occupancies of proton levels vary more smoothly across the Fermi surface, a consequence of increased correlations. The present observations and those of Gade *et al.* [5] can be understood from the larger strength of p-n relative to the p-p and n-n interactions. Hence, protons (neutrons) experience larger (weaker) correlations in neutron-rich matter. The reversed is true for proton-rich matter.

This work was supported by the U.S. Department of Energy, Division of Nuclear Physics under Grant No. DE-FG02-87ER-40316.

[1] W. H. Dickhoff and C. Barbieri, Prog. Part. Nucl. Phys. **52**, 377 (2004).
[2] G. Colò, P. F. Bortignon, and R. A. Broglia, Nucl. Phys. **A649**, 335 (1999).
[3] V. R. Pandharipande, I. Sick, and P. K. A. de Witt Huberts, Rev. Mod. Phys. **69**, 981 (1997).
[4] D. Rohe *et al.*, Phys. Rev. Lett. **93**, 182501 (2004).
[5] A. Gade *et al.*, Phys. Rev. Lett. **93**, 042501 (2004).
[6] C. Mahaux and R. Sartor, Adv. Nucl. Phys. **20**, 1 (1991).
[7] W. H. Dickhoff and D. Van Neck, *Many-Body Theory Exposed!* (World Scientific, New Jersey, 2005).
[8] C. B. Fulmer *et al.*, Phys. Rev. **181**, 1565 (1969).
[9] J. F. Dicello *et al.*, Phys. Rev. C **4**, 1130 (1971).
[10] W. T. H. Van Oers, Phys. Rev. C **3**, 1550 (1971).
[11] A. Nadasen *et al.*, Phys. Rev. C **23**, 1023 (1981).
[12] H. Sakaguchi *et al.*, Phys. Rev. C **26**, 944 (1982).
[13] R. H. McCamis *et al.*, Phys. Rev. C **33**, 1624 (1986).
[14] L. N. Blumberg *et al.*, Phys. Rev. **147**, 812 (1966).
[15] R. M. Graig *et al.*, Nucl. Phys. **86**, 113 (1966).
[16] D. L. Watson *et al.*, Nucl. Phys. **A92**, 193 (1967).
[17] V. Hnizdo *et al.*, Phys. Rev. C **3**, 1560 (1971).
[18] P. Schwandt *et al.*, Phys. Rev. C **26**, 55 (1982).
[19] H. S. Liers, Nucl. Phys. **A170**, 616 (1971).
[20] J. C. Lombardi *et al.*, Nucl. Phys. **A188**, 103 (1972).
[21] W. Bauhoff, Atom. Data Nucl. Data Tables **35**, 429 (1986).
[22] G. J. Kramer *et al.*, Phys. Lett. B **227**, 199 (1989).
[23] G. J. Kramer, H. P. Blok, and L. Lapikás, Nucl. Phys. **A679**, 267 (2001).
[24] D. J. Millener and P. E. Hodgson, Nucl. Phys. **A209**, 59 (1973).
[25] W. Tornow, Z. P. Chen, and J. P. Delaroche, Phys. Rev. C **42**, 693 (1990).
[26] R. L. Varner *et al.*, Phys. Rep. **201**, 57 (1991).
[27] A. N. James *et al.*, Nucl. Phys. **A138**, 145 (1969).
[28] G. A. Rijsdijk, K. Allaart, and W. H. Dickhoff, Nucl. Phys. **A550**, 159 (1992).
[29] T. Frick *et al.*, Phys. Rev. C **71**, 014313 (2005).
[30] D. H. Youngblood *et al.*, Phys. Rev. C **2**, 477 (1970).
[31] P. Doll *et al.*, Nucl. Phys. **263**, 210 (1976).
[32] J. W. Watson *et al.*, Phys. Rev. C **40**, 570 (1989).